Brazilian Journal of Geophysics 40 (2022), 3, 431-443
Brazilian Geophysical Society
ISSN 2764-8044
DOI: 10.22564/brjg.v40i3.2176

Potentiometric and Bedrock Map Drawn from Vertical Electrical Soundings (VESs) and Considerations on the Investigation Depth

José Domingos Faraco Gallas

Universidade de São Paulo – USP, Dep. Geologia Sedimentar e Ambiental, Inst. Geociências, São Paulo, SP, Brazil

Corresponding author e-mail: jgallas@usp.br

ABSTRACT. The article presents considerations on the depths achieved by Vertical Electrical Soundings (VESs) as a function of electrode distances and also on their quantitative interpretation. Besides the distances among electrodes, the effective achieved depths will depend on the resistivity distributions. At the request of environmental agencies, resistivity geophysical surveys were carried out in an area designed to the implementation of a residential complex, which would have to present a site hydrogeological study, including a potentiometric map among other requirements to be met. For the referred map elaboration, 18 VESs were carried out in order to determine the depth of the water level at these points. In addition to this information, the works provided another additional data: the determination of the bedrock depth. Based on the VES results, the potentiometric map and the bedrock depth map were elaborated in the study area. The cost reduction with the use of this indirect technique is significantly lower when compared to the costs of mechanical soundings, besides the reduction of the execution time.

Keywords: vertical electrical sounding; potentiometric map; bedrock map.

INTRODUCTION

Groundwater aquifers are susceptible to anthropic interventions, and this is one of the reasons for local hydrogeological studies to be carried out, in order to adopt measures that minimize any damage to them.

In situations of enterprises such as the one in the present situation (implementation of a housing complex) environmental agencies usually request hydrogeological studies among other requirements.

The local hydrogeological study of detail (potentiometric map, in this case) can be obtained by drilling wells to determine the saturated medium depths at various points. Or, as in here, it can also be accomplished through VES execution. It is an indirect technique, but with lower costs, faster and with sufficient precision for this purpose.

Therefore, this geophysical survey had a fundamental purpose of indirectly estimating the water table depth in order to make a potentiometric map for the area of interest. The study mainly aimed at determining the resistivity patterns that could be correlated to the saturated layer top. Secondly, a map with the bedrock depth was also obtained. For this purpose, 18 VESs were carried out and parameterized by direct information obtained by measuring the water level depths in two dug wells existing in the studied area.

The main reason for the elaboration of the potentiometric map by using the VES was the low cost of this type of work, when compared to the costs and execution time of mechanical drilling. In areas where the water level is shallower (depths smaller than 4-5 m), it would be more appropriate, and with reasonable costs and times, to obtain the water table depths through sounding. In the present situation, where the water level is between 6 and 19 m, the costs are lower and the time spent to obtain the results is significantly lower, in addition to obtaining an additional data, namely bedrock depth.

GEOLOGY

Locally and superficially, the altered soil plus rock part, the most relevant for this work purposes, has a thickness ranging from 39 to 49m, as indicated by the VES carried out here.

During the geophysical survey campaign, field inspections found outcrops of granite-gneiss rocks in the vicinity of the area of interest.

In fact, according to the bibliography on geology in which the work area is included, this is a pre-Cambrian crystalline basement whose rocks belonging to the Amparo Complex, Socorro Domain, and Atibaia Granitic Massif occur. Restrictedly, there are Cenozoic sedimentary coverings.

As Hasui and Oliveira (1984) redefined, the Amparo Complex corresponds to Amparo, Itapira and Socorro units, mainly consisting of metamorphic rocks, gneisses, schists and granitoids or granite-gneisses (Etchebehere et al., 2007).

The Socorro Domain has its lytic constitution ranging from porphyritic rosy to equigranular granites, fine-grained rosy granites, inequigranular to equigranular, white, hololeucocratic and porphyritic (Etchebehere et al., op cit.).

The Atibaia Granite is quite homogeneous, being the granite types that constitute it composed of quartz, microcline, oligoclase, biotite and hornblende. Its granulation is medium to coarse, reaching very coarse, usually inequigranular, with the predominant rosy coloration. Locally, it may occur an increase in xenoliths of gneissic composition (Etchebehere et al., op cit.).

APPARENT RESISTIVITY (PA)

The parameters involved in resistivity surveys are the current ***I*** obtained from a ***E*** source emitted through two electrodes ***A*** and ***B*** in galvanic contact with the soil and the difference in ***ΔV*** potential observed in two electrodes of ***M*** and ***N*** potential.

Knowing the positions of these four points on the ground, it is possible to obtain the ***ρ*** resistivity. Assuming a homogeneous and isotropic terrain, this resistivity would be the same for any provisions of *A, B, M, and N*. However, the general rule is that the soils / subsoils are neither homogeneous nor isotropic, and, most often, *A, B, M and N* are placed in locations of different resistivity. Under these conditions, the measured resistivity will not be true but a ρ_{an} apparent resistivity involving the contribution of all ones. This final measured resistivity should not be considered as an average or weighted mean of the involved resistivities, and it is possible to be greater or lesser than any of them (Orellana, 1972).

For the calculation of these resistivities, it is considered a semi-space (2π geometry) from the land surface to the subsoil (Keller and Frischknecht, 1966). Also, it is employed a ratio in which two current sources (**A** and **B**) and two measurement points (**M** and **N**) are considered, as shown in Figure 1.

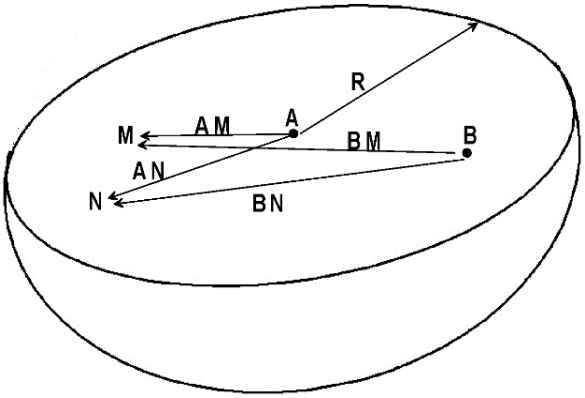

Figure 1: Semi-space with two current sources and two measurement points.

By conventionalizing the potential in **B** negative and assuming that the current goes into **A** and comes out in **B**, there is the ratio for the calculation of resistivities (simplified by Keller and Frischknecht, 1966)

$$\rho_a = \left(\frac{V_M - V_N}{I}\right)\frac{2\pi}{\frac{1}{AM} - \frac{1}{BM} - \frac{1}{AN} + \frac{1}{BN}} = K\frac{\Delta V}{I}$$

And synthesizing

$$\rho_a = K\frac{\Delta V}{I}$$

Where K is the geometric factor that depends on the distances between the current and potential electrodes involved in the measurement.

Vertical Electrical Sounding (VES)

Vertical Electrical Sounding is a technique in which a series of apparent resistivity measurements are made, carried out with increasing separation between emission electrodes **A** and **B** (Figure 2). The VES purpose is the vertical determination of resistivity below the point of interest.

By increasing the distance between the current electrodes **A** and **B**, the total subsurface volume included in the measure also increases, which allows reaching deeper and deeper layers. The results will therefore be strictly linked with variations in resistivity with depth (ρ_1, ρ_2,... ρ_n).

The data obtained in each VES are represented by means of an apparent resistivity curve as a function of distances between the electrodes and are processed and interpreted by using abaci and / or automatic 1D inversion programs (one-dimensional).

Under ideal conditions, the VES should be performed on a terrain composed of laterally homogeneous layers (in relation to resistivity) and limited by planes parallel to the terrain surface (stratified medium). The results are tolerably valid for slopes of these layers up to 30º.

The Schlumberger array (Figure 3) is the most used VES. It consists of two electrodes for the transmission of current ***A*** and ***B*** and two potential electrodes ***M*** and ***N*** for the reading of potential difference measures, aligned on the same survey profile, and the ratio between ***AB / MN ≥ 5***. The VES development is due to the progressive distance of the current emission electrodes ***A*** and ***B*** (***L, L', L"***...etc.). The center ***O*** is fixed and the distance between the ***MN*** electrodes should also be kept constant as long as possible, at least the providing of the signal reception is suitable. When the ΔV signal becomes too weak, it can increase the distance ***MN*** by making the due "clutch" (clutch = repetition of the ΔV reading with two or more MN distances for the same AB distance).

The measurement plot point is the midpoint ***O*** between ***M*** and ***N***, and the results are presented in the form of resistivity curves, plotted in bi-logarithmic graphs. The plotting of the apparent resistivity measures is made on the ordinate and abscissa axes, AB / 2 distances.

The plotting system in bi-logarithmic graphs is adopted because the ratio between the resistivities is the most important and not the difference between them (the number of measurements is usually the same per logarithmic decade of AB distances). For example, a difference of 100 Ω.m is significant when resistivities are of 200 Ω.m, but it becomes almost irrelevant if the values are around 3,000 or 4,000 Ω.m. Thus, this plotting system highlights the variations of the most important geoelectric strata.

Brief Literature Review

There are several articles in the literature that deal with the VES technique application for objectives similar to those presented here. The ones that fit these objectives are those that aim to determine the vertical resistivity variations, and when interpreted results they allow to establish the appropriate geological / geophysical correlation. The technique is particularly effective for flat-stratified media, such as determining geoelectric strata thicknesses of geoelectric layer type and water level and bedrock detection, as in the present case.

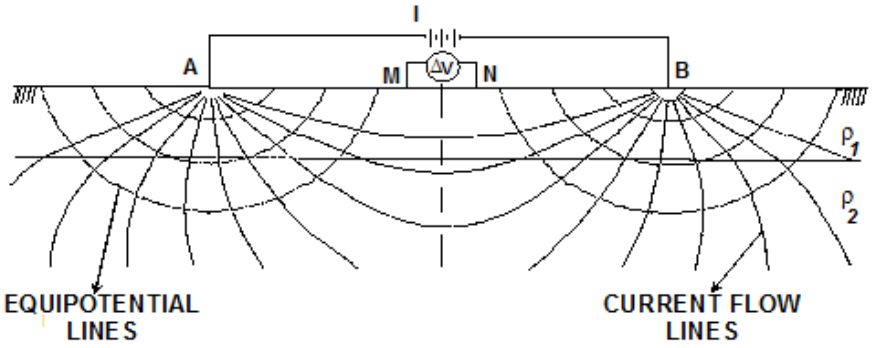

Figure 2: Illustration of electrode configuration for VES technique.

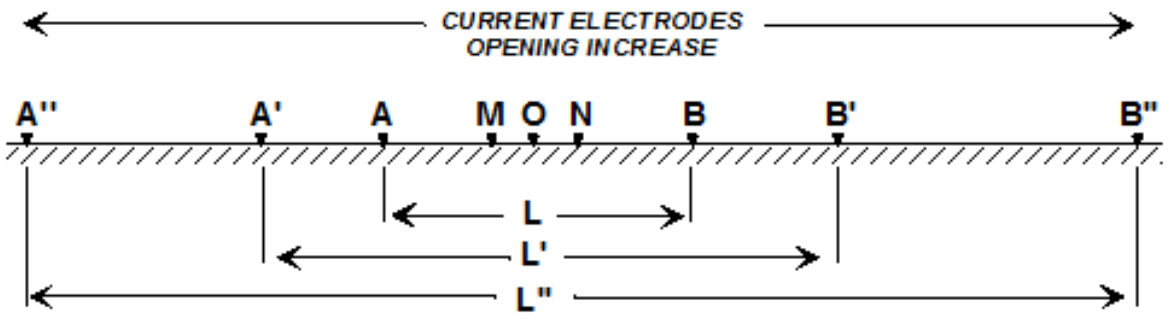

Figure 3: Schlumberger array.

One of this use cases is the Cutrim and Rebouças (2005) work. They estimated the top and thicknesses of the geological strata in Paraná Basin. A pioneering study, such as the Roy and Apparao (1971) work, is also mentioned. They already dealt with the quantification of the effective depths of investigation by resistivity.

Furthermore, with similar purposes, to indirectly quantify the depths / thicknesses of geoelectric strata, some works can be mentioned, namely Cutrim et al. (2007), Leal (2007), Oliva and Chang (2007) and Cutrim and Shiraiwa (2011).

Silva (2014), using electric walking (dipole-dipole) and VES techniques, characterized an area aiming to select intact rocks (without fractures) and with little alteration mantle for extraction of large granite blocks.

Binley and Slater (2020) address the geoelectrical methods of resistivity and induced polarization (IP) for shallow investigations in hydrogeology, engineering geology, archeology, etc. and present a software (open-source) for processing these data.

Rucker et al. (2021) applied resistivity and IP for investigations smaller than 15m to determine, mainly, the soil / rock (limestone) interface.

DEPTH OF INVESTIGATION

One of the most discussed aspects in resistivity is the depth of applied-current and electric-field penetration that will determine the achieved depth of investigation. This fact has its greatest importance in VES case, where the specific array purpose is this information quantification.

The depth of investigation can be defined as the depth at which a target is detected by a given electrode configuration. In principle, there should be a close relation between electrode spacing and type of array with the effective depth of investigation aimed at solving a really complex problem.

The first to define the depth of investigation, Evjen (1938), uses the concept "depth factor" that relates a distance measured on the surface (considering the distance between electrodes) with the depth. Apparent resistivity measurements result from the integration of the entire investigated package. It is a kind of weighted average of the resistivity contained in the total volume, with different weights for each package (thickness and resistivity) stratum. As a result, the depth factor would be the depth of the stratum presenting greatest measure and expressed contribution as a fraction of the distance between electrodes. This author defines the depth of investigation as being that in which half of the total current is located above a geoelectric interface and the other half below it, also emphasizing that the penetration depends on the distribution of electrical properties of the medium with depth.

Roy and Apparao (1971) establish the depth of investigation as one in which a thin horizontal layer contributes the maximum of the total measurement detected on the surface. Table 1 shows these depths where L is the distance between the extreme electrodes of the array.

Table 1: Depths of investigation according to Roy and Apparao (1971).

Electrode Configuration	Depth
Wenner	0.11 L
Dipole-dipole	0.195 L
Schlumberger	0.125 L

In Table 2, $\boldsymbol{L}$ is the distance between the extreme array electrodes; $\boldsymbol{a}$ is the distance between measurement electrodes (potential); and $\boldsymbol{x}$ is the distance between the center of the potential electrodes and the nearest current electrode.

Based on Roy and Apparao (1971), Roy (1972) and Edwards (1977), Barker (1989) established depth of investigation values for some electrical arrays (Table 3).

Edwards (1977) defines that the effective depth is determined by both the position of both current and potential electrodes. The algorithm used in the IP-resistivity inversion software (Res2DInv) is based on the depths proposed by Edwards (1977), but which can be modified by the user.

Following the same line of studies, comparing conductive and resistive targets, Apparao et al. (1997) concluded that the detection depth for such targets is comparatively lower for resistors than for conductive ones. That is, it is not only the distances between electrodes and arrays that are involved but also the main variable of interest, resistivity. Furthermore, all these mentioned authors conducted these studies not only for resistivity, but also for induced polarization (IP).

In a real case of mineral prospecting using IP-resistivity, Gallas (2000) found that the detection depth of a mineralization for dipole-dipole was between Hallof (1957) and Edwards (1977) depths, a fact proven by a sounding that intercepted the top of a sulphide

mineralization at a depth of 34 m (for dipole-dipole array with AB=MN=50m and 5 levels).

Table 4 presents the comparative data of this case. The results showed that the mineralization response (Cu, Pb, and Zn) was of high chargeability (IP) and low resistivity. The depths correspond to the first level of investigation (n=1 and electrode spacing AB=MN=50 m), and the depth that the sounding intercepted at the top of the mineralization.

Using simple (cylindrical and tabular) and porous geometric models, with dipole-dipole (mainly) and Wenner (Gallas and Verma, 2006; Gallas, 1990) in analog modeling, in laboratory-developed analog modeling under fully controlled conditions, it is showed that the target detection depth can be even greater than the Hallof (1957) depth. The measured parameters were Vp (primary voltage), RPS (Relative Phase Shift) and PFE (Percentage Frequency Effect). Figure 4 illustrates the result obtained for tabular model with 2 x 30 x 30 cm and cylindrical model with 2.54 cm in diameter and 30 cm in length, built with sand, graphite, and cement. The models were immersed in a water solution with a concentration of 2.55 x 10^{-4} CuSO4 g / L and resistivity of 1221 Ω. m. The electrodes were Pt and the graphite (contents of 10, 20 and 30 %) was used to simulate the presence of metallic sulfides (30% content in the modeling presented here). The parameter displayed in Figure 4 is the primary voltage (Vp). As measurements were always taken every 2 cm (dipole-dipole with AB=MN=2cm), and constant current, the Vp measurement has the same meaning as resistivity. In addition to this modeling, dozens of others were partially presented in Gallas and Verma (2006) and their full version is in Gallas (1990). The models were placed at depths of 0.5, 1.0 and 2.0 cm.

Hallof (1967, 1968, and 1970) also performed analog modeling for IP-resistivity in the laboratory for hundreds of models and situations and corroborated the depths Hallof (1957) proposed. Reduced models were constructed with: 1) gelatin with copper sulfate; 2) gelatin and gypsum with copper sulfate, and 3) graphite and carbon powder. The models were immersed in a tank with water whose resistivity could be varied by modifying the salinity. The measurement electrodes (stainless steel) were placed at the bottom of the tank. Figure 5 brings the original data (the original data were typed and reinterpolated from the original Hallof figure without inversion processing.) from one of the Hallof (op cit.) models to a tabular model of dimensions: width=0.25 units; length=1.85 units, and extension=1.6 units. The model was positioned at a depth of 1.0 unit from distances between the electrodes (AB=MN=1.0). Figure 5 shows only the resistivity section (ρ).

In a critical comparative analysis of 14 factors that must be considered when choosing an electrode array (attributing the value "1" to very favorable and "5" to an unfavorable situation), in the item "penetration depth", Ward (1990) does not make this assessment, justifying the uncertainties in the estimation of this parameter for the evaluated electrode arrays.

Table 2: Depths of investigation as a function of L for gradient, Wenner and Schlumberger, according to Edwards (op. cit.)

Gradient Depth		**Wenner Depth**	**Schlumberger Depth**	
L = 40a; x = 20a	0.192 L	0.173 L	L = 40a	0.192 L
L = 40a; x = 15a	0.163 L		L = 20a	0.191 L
L = 40a; x = 10a	0.103 L		L = 10a	0.190 L

Table 3: Depths of investigation, according to Barker (1989).

Electrode Configuration	**Depth**
Wenner	0.17 L
Schlumberger	0.19 L
Dipole-dipole	0.14 L

Table 4: Depths of investigation for dipole-dipole and sounding.

Author	**Depth (n=1)**
Hallfof, 1957 (L/2)	50m
Roy and Apparao, 1972 (0.195 L)	29.5m
Edwards, 1977 (0.139 L)	20.85m
Barker, 1989 (0.14 L)	21m
Drilling	**34m**

In fact, the achieved depth of investigation will depend on the behavior of the subsurface resistivity distributions. The presence of a superficial conductive layer (clayey mantle, saturated and / or salinized alteration) will significantly reduce the current penetration, resulting in a thickness decrease of the investigated package. A highly resistive package (e.g., anhydrite, lateritic crusts) can also be a barrier to current penetration, hindering or preventing, equally, the continuity of the investigation.

In most practical situations, the distribution of the underlying lithologies and their physical properties (resistivity, in this case) are unknown, and a starting point may be to establish as an initial model a homogeneous and isotropic semi-space. In heterogeneous mediums, the current density will differently fluctuate in each medium, being at the mercy of resistivity distributions. Thus, it is not possible to establish in advance which depth of investigation will be achieved, regardless of the used electrode array. Especially in the case of vertical electrical sounding (VES), the depth investigated will depend on the resistivity distribution of different geoelectric strata, their thicknesses, and the order of alternation between resistive and conductive strata.

Finally, the detection of a geoelectric stratum in a VES will be given by the curve inflection in the resistivity x AB / 2 graph, which will tend to another resistivity, greater or lesser than the overlying one. This inflection will occur when the electric current penetrates the underlying stratum, and the measurements suffer a noticeable contribution of it. This inflection may occur before or after the half of the total current is located above, and the other half located below it (Evjen, 1938; Muskat and Evinger, 1941; Edwards, 1977). It will happen before when the contrast of resistivities between the layers is large and, consequently, will occur later if the contrast is small.

Thus, a "detection depth" for a lithological change (or resistivity) does not necessarily imply that for this half of the current the propagation above this interface and, for the other half, below it. It seems reasonable to state that this "detection depth" will be effective if a resistivity contrast is detectable when a measurable change in measurements occurs.

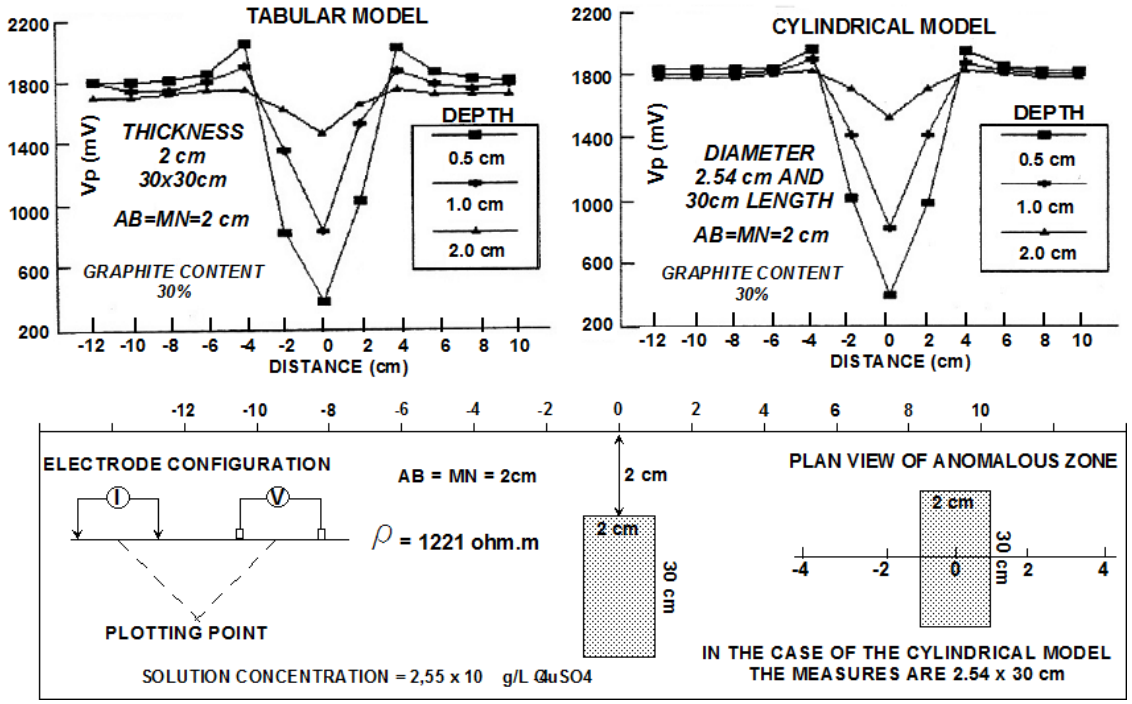

Figure 4: Resistivity response with increasing of investigated depth (Gallas 1990; Gallas and Verma, 2006).

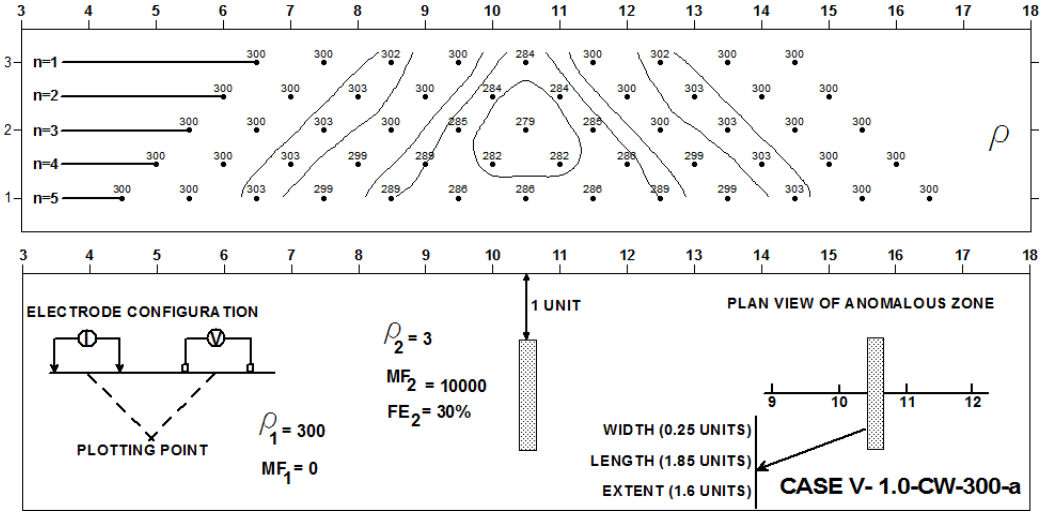

Figure 5: Original by Hallof (1967, 1968, 1970) CASE – 1.0-CW-300-a.

Table 5: VESs, AB distances, UTM coord., and synthesis of interpretations (considering water level –water table– depths and sound rock depths).

COORD. A	COORD. N	VES	TOTAL AB (m)	VES QUOTA (m)	NA VES (m)	QUOTA NA (m)	BEDROCK (m)
320634	7437346	VES-01	260	808.4	10.0	798.4	48.0
320791	7437274	VES-02	260	812.2	10.2	802.0	44.0
320842	7437174	VES-03	400	816.4	13.0	803.4	43.0
320928	7436993	VES-04	260	821.3	13.8	807.5	40.0
320708	7437291	VES-05	320	815.5	11.8	803.7	45.0
320778	7437097	VES-06	400	833.4	16.5	816.9	41.0
320882	7436951	VES-07	260	834.7	16.8	817.9	40.5
320436	7437263	VES-08	260	793.3	6.0	787.3	49.0
320441	7437169	VES-09	320	802.5	8.5	794.0	47.0
320421	7437066	VES10	260	807.7	10.0	797.7	46.0
320390	7436912	VES-11	320	807.2	10.5	796.7	45.5
320432	7436834	VES-12	200	817.3	13.0	804.3	42.0
320468	7437005	VES-13	400	821.0	14.0	807.0	42.5
320510	7437171	VES-14	400	817.9	12.9	805.0	44.0
320574	7437098	VES-15	260	831.4	15.7	815.7	41.0
320556	7436929	VES-16	400	841.6	18.0	823.6	39.5
320718	7437160	VES-17	320	832.5	16.2	816.3	41.5
320741	7437002	VES-18	400	847.8	19.2	828.6	39.0
320543	7437257	Dug Well	xxx	817.0	12.6	804.4	xxx

RESULT INTERPRETATION AND ANALYSIS

Basically, the geophysical characterization expected to achieve the objectives of this research is that the saturated level (groundwater / water level) is evidenced by a drop in resistivity. On the other hand, the bedrock (rocks of granitic-gneissic composition) will present greater resistivity than the geoelectric stratum that is overlaid on it.

The VESs were interpreted according to automatic 1D inversion processes where, from the apparent resistivity curves, a geoelectric model is established for each VES and can correlate it with the geology of the studied area (Zhody, 1989). The used software for the inversion was *IPI2WIN (2000), Resistivity Sounding Interpretation, version 3.1.2c, Moscow State University*.

To obtain a more accurate interpretation, VESs were parameterized from 2 points that provided water level depth data. The first of these was in the vicinity of VES-08, where there is a dug well in which the water level was measured at 1.30 m. The VES-08 is a neighbor of it, but with an altitude of 4.70 m higher. From this parameterization, a depth of 6.0 m for the water table was interpreted in this VES.

The other water level point known and used in the making of the potentiometric map was the *dug well* point, referred to in Figures and Table 5, whose coordinates are 320543E and 7437257N, elevation of 817 m, and measured water level depth equal to 12.60 m.

Figure 8 presents the potentiometric map and was elaborated from the results obtained and interpreted in 18 VESs performed in the area. In the potentiometric map, flow gradient vectors were inserted, represented by blue arrows, indicative of the directions of the subsurface water flows.

Initially, this geophysical survey purpose was to estimate the water table depth. However, the obtained data provided a very important additional information, which was the bedrock depth, presented in Figure 9.

All VESs were interpreted according to a geoelectric model very similar and common to all, which consists of 5 (or 6) layers. The interpreted model can be synthesized as:

- **1st geoelectric stratum:** dry or partially saturated, with high resistivities.
- **2nd geoelectric stratum:** idem, but the resistivity is a little lower; in some cases, considered as saturated and top of the water level.
- **3rd geoelectric stratum:** less resistive, in some VESs interpreted as the beginning of the water level.
- **4th geoelectric stratum:** the lowest resistivity; also, in some VESs interpreted as the water level.
- **5th geoelectric stratum:** interpreted as being the bedrock, end of the soil and altered rock package, and beginning of the healthy rock.
- **6th geoelectric stratum:** when there is a need to include the sixth layer for the best data adjustment, this sixth stratum is only a subdivision of one of the 5 layers and does not interfere with the quantification of the main objects of interest, which are the water level and the bedrock depth.

As expected, the VES curves show that the water level characterization is given by a drop in the resistivity values. As in nature, the electric current propagates mainly in an ionic way (Gallas, 2000 *apud* Keller and Frischknecht, 1966), then it is expected that the presence of water saturating the subsoil facilitating the ion dissolution and mobility, provides a consequent drop in resistivity. These resistivity drops identified in the VES curves allow them to be attributed to water level.

At the end of the VES curves, the identification of a more resistive geoelectric stratum is attributed to the healthy rock (granite-gneiss) which, due to its intrinsic characteristics of very low porosity, virtually contains no dissolved ions, and will consequently have higher resistivity.

RESULT PRESENTATION

With the main objective to estimate the depths of the water level top, and, secondarily, the bedrock depth, 18 VESs were performed. The VESs were distributed in order to cover the area of interest in the best possible way, forming a sampling mesh appropriate to the work purpose. The results are synthesized as maps. The curves and interpretations of 8 from the 18 VESs performed are also presented.

Figure 6 shows the VES locations overlapping a Google Earth image. Figure 7 shows a view (obtained via Google Earth Street View) of the studied area.

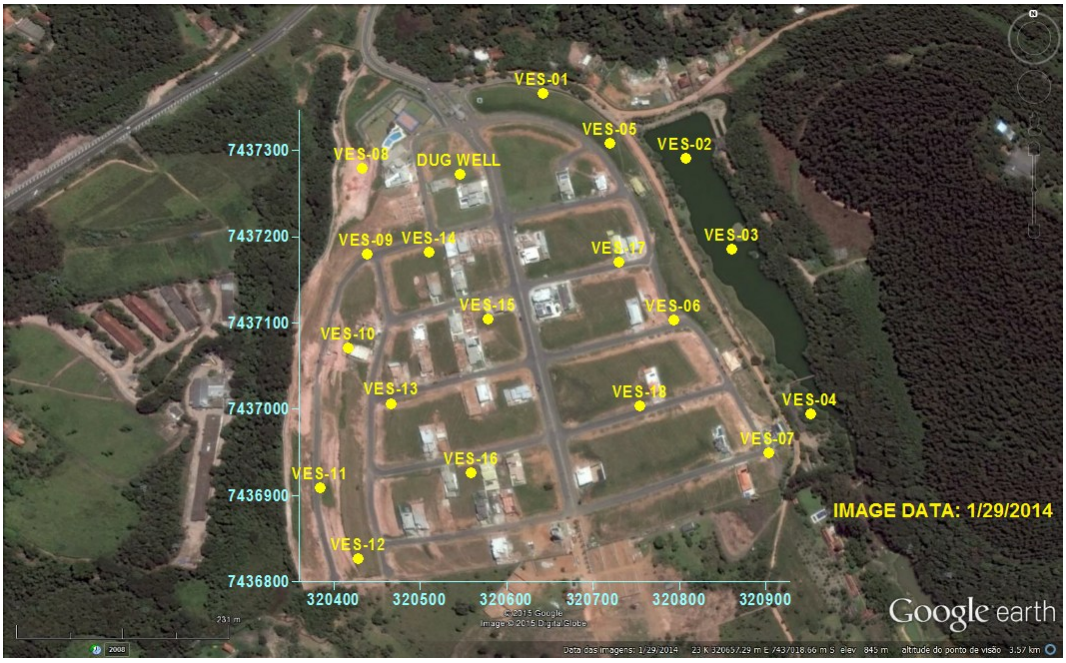

Figure 6: Google Earth image and VES location in the area.

Figure 7: Google Earth image (Street View) with the area view.

Figure 8 shows the main result of this research: The potentiometric map, elaborated from water level depths quantitatively interpreted from the VES bi-log curves.

Figure 9 presents the obtained by-product, a map of the bedrock (healthy rock) depth. The lithology from the studied area is of granite-gneissic composition.

Figures 10 to 17 show the bi-logarithmic graphs of the VESs 1, 2, 5, 6, 7, 13, 14 and 16 VES, in this order, with their respective quantitative interpretations. The meaning of the symbology in Figures 10 to 17 is as follows:

o = resistivity measured in the field.

black line = field curve.

red line = curve modeled by the inversion software.

ρ = resistivity.

h = geoelectric stratum thickness.

d = depth of the geoelectric stratum base.

Alt = altitude of the stratum base in relation to the surface.

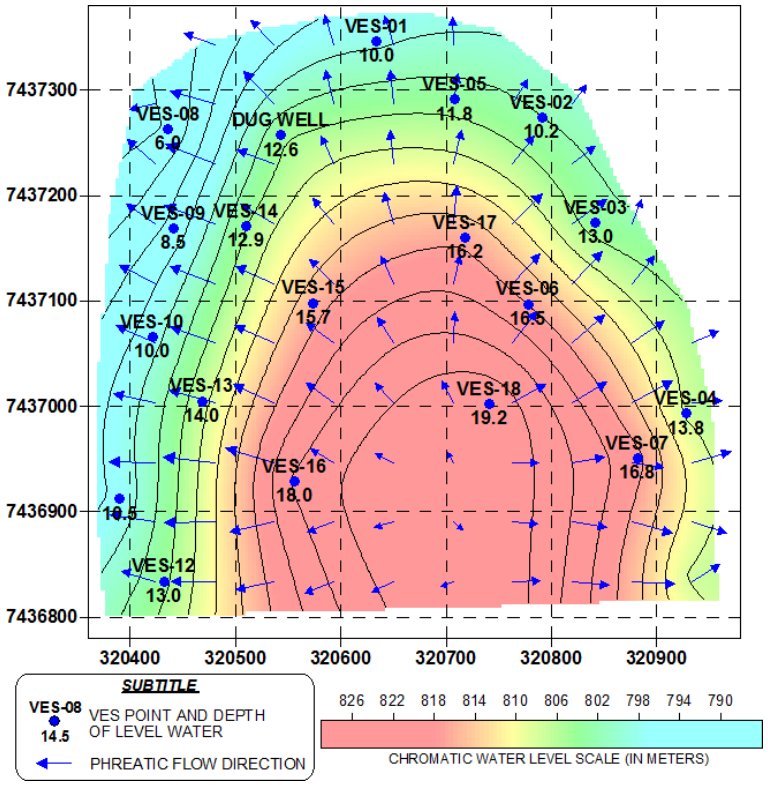

Figure 8: Potentiometric map. Shows the main result of this research: The potentiometric map, elaborated from water level depths quantitatively interpreted from the VES bi-log curves.

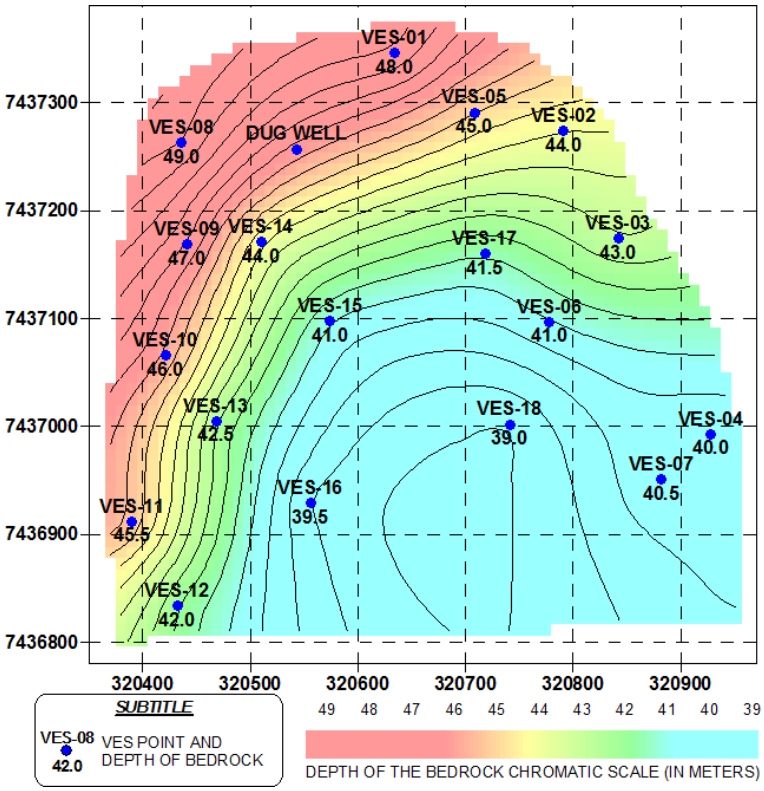

Figure 9: Bedrock depth map. Presents the obtained by-product, a map of the bedrock (healthy rock) depth. The lithology from the studied area is of granite-gneissic composition

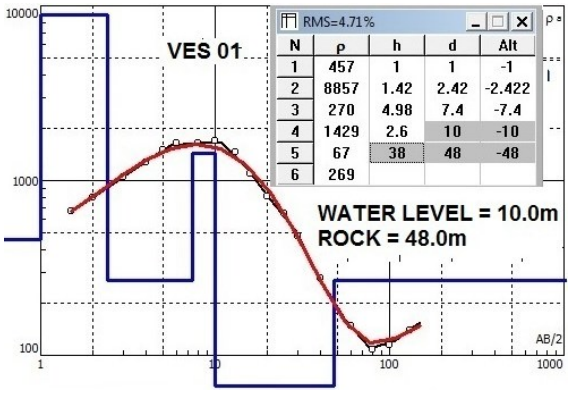

Figure 10: Interpreted VES-01.

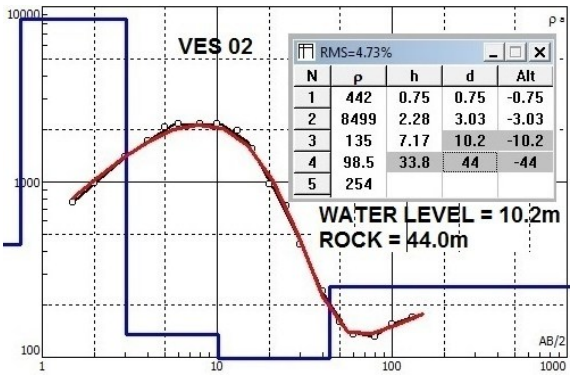

Figure 11: Interpreted VES-02.

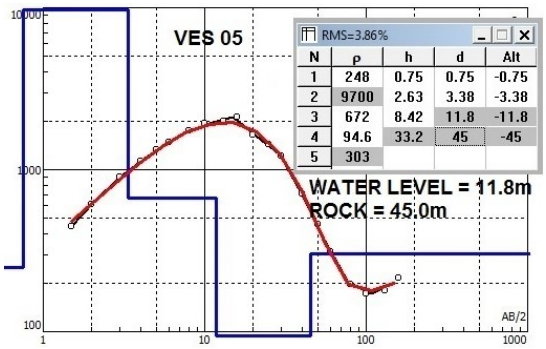

Figure 12: Interpreted VES-05.

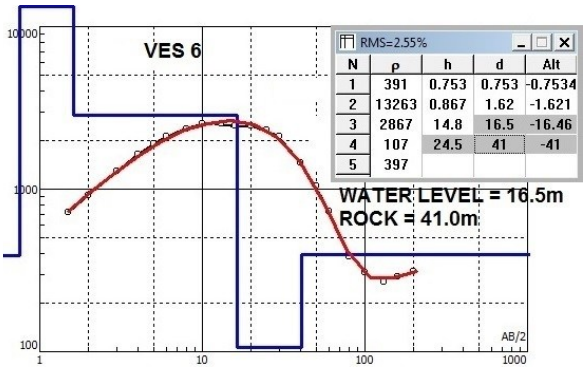

Figure 13: Interpreted VES-06.

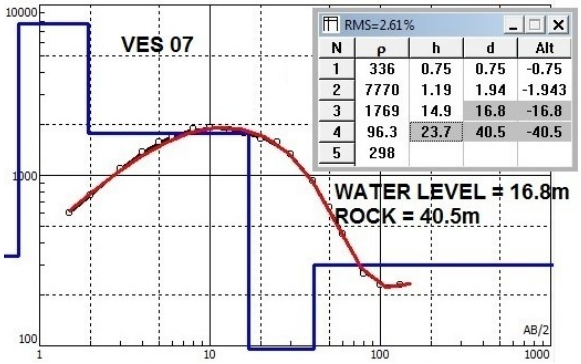

Figure 14: Interpreted VES-07.

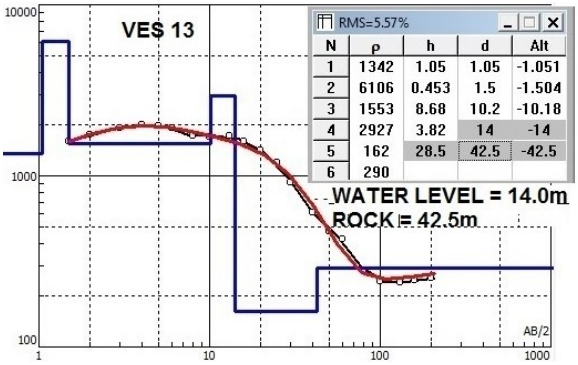

Figure 15: Interpreted VES-13.

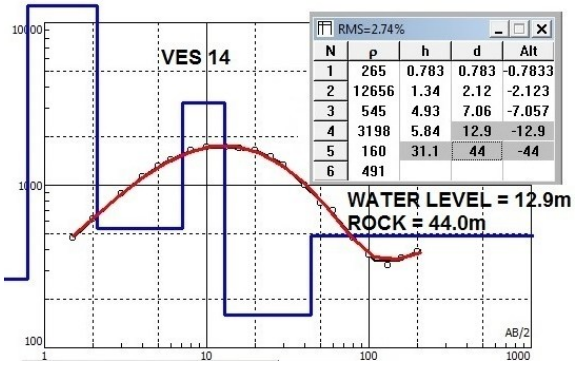

Figure 16: Interpreted VES-14.

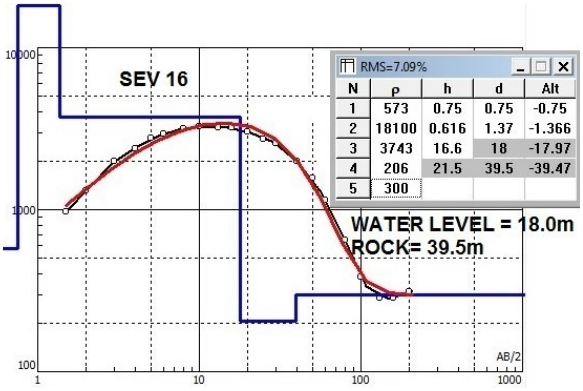

Figure 17: Interpreted VES-16.

CONCLUSIONS

The resistivity method and the VES technique are geophysical tools of indirect prospecting. In order to optimize their results, it is always desirable they can be parameterized by direct information. In the present case, this was done with information data from two points whose groundwater depth was measured.

The depth of investigation VES achieved will depend on the subsurface resistivity distributions. The presence of a superficial conductive layer will significantly reduce the current penetration, reducing the investigated package thickness. A very resistive package can also be a barrier to current penetration as well as to the continuity of the research. It is worth remembering that the geological layers do not always coincide with the geoelectric strata.

A priori, the distribution of the geoelectric strata and their resistivity are unknown. In heterogeneous media, the current density will be different in each of them, and it is not possible to pre-establish which depth of investigation will be achieved. The investigated depth will depend on the distribution of the resistivities of different geoelectric strata, their thicknesses, and the alternation order between more resistive and less resistive strata.

The change from one geoelectric stratum to another in a VES is detected by the curve inflection in the resistivity graph x AB/2, which will tend to another resistivity, greater or lesser than the overlying one. This occurs when the electric current penetrates the underlying stratum, and the measurements suffer a noticeable contribution of it. This inflection may occur before or after half of the total current is located above and the other half is located below it (according to several authors). It will happen before when the contrast of the resistivities between the layers is large and it will occur later if the contrast is small, implying different investigated effective depths.

The assumed premises (the saturated level –water table / water level – is indicated by a drop in resistivity and the bedrock – rocks of granite-gnaissic composition– presents greater resistivity) were confirmed, allowing the VES interpretation to provide the obtained good results.

The VESs were interpreted by establishing a geoelectric model very similar and common to all, which fits in the data inversion processes with 5 (or 6) layers. The maps elaborated for the studied area allowed obtaining the distributions of the water table and bedrock depths, as well as the water flow gradient vectors evidencing their preferred directions.

Another aspect to be considered is the one which refers to costs and time. The field time for execution of the 18 VESs was 04 days, including daily round trips to the area, lasting from 2 to 3 hours. If instead of VES carrying out mechanical sounding for the water level determination at the verified depths (between 6 and 19 m, and in only 2 of 18 the water table is less than 10 m), the costs and execution time would be much higher. Furthermore, if it were for bedrock (between 39 and 49 m) determination, then the costs and execution time would be even much higher and even prohibitive, because in this case it would imply to even higher costs in rotating surveys. Auger drilling (manual or mechanical) costs can vary from R$80 to R$150 per drilledmeter (approximately US$15 to US$28 per meter, respectively). Besides, if the drilling depths are greater than 20-25m, the use of rotary drilling will be necessary, and the cost per meter will be around R$ 500 (US$ 93, approximately). Also, there is the need to add the mobilization fee (varying according to location and distance).

On the other hand, in situations where the water level is shallower (less than 4 or 5 m), the obtaining of water table depths through auger sounding may be more indicated, with reasonable costs and time.

The results presented here allow concluding that the proposed objective was achieved, which is to determine the depth of the top of the water level at various points in the area, allowing the construction of the local potentiometric map. In addition, the obtained data interpretation provided other relevant information, which was the bedrock (top of healthy rock) depth, providing the elaboration of a map of this parameter for the object area.

REFERENCES

Apparao, A, R. S. Sastry, and V. S. Sarma, 1997, Depth of detection of buried resistive targets with some electrode arrays in electrical prospecting: Geophysical Prospecting, **45**, 365–375, doi: 10.1046/j.1365-2478.1997.3360256.x.

Barker, R. D., 1989, Depth of investigation of collinear symmetrical four-electrode arrays: Geophysics, **54**, 8, 1031–1037, doi: 10.1190/1.1442728.

Binley, A., and L. Slater, 2020, Resistivity and Induced Polarization: Theory and Applications to the Near-Surface Earth. Cambridge: Cambridge University Press. 408 pp. doi: 10.1017/9781108685955.

Cutrim, O. A., and A.C. Rebouças, 2005, Aplicação de sondagem elétrica vertical na estimativa do topo e da espessura de unidades geológicas da bacia do Paraná na cidade de Rondonópolis, MT. Revista Brasileira de Geofísica, **23**, 1, 89–98, doi: 10.1590/S0102-261X2005000100008.

Cutrim, A. O. and Shiraiwa, S., 2011, Prospecção de Água Subterrânea no Sudoeste do Município de Rondonópolis (MT) Usando Sondagem Elétrica Vertical: Revista Brasileira de Geofísica, **29**, 4, 745–751, doi: 10.22564/rbgf.v29i4.78.

Cutrim, A. O., Ruiz, A. S., Liporoni, L. M., Medeiros, F. A., Barroso, U. C, and Nascimento, A. L., 2007, Sondagem elétrica vertical aplicada em pesquisa hidrogeológica na Bacia do Parecis, MT: Revista Brasileira de Geofísica, **25**, 131–140, doi: 10.1590/S0102-261X2007000200003.

Edwards, L. S., 1977, A modified pseudo section for resistivity and induced-polarization: Geophysics, **3**, 78–95.

Etchebehere, M. L, A. R. Saad, Bistrichi, C. A, Garcia, M. J, Silva, M. F, and Bedani, E. F., 2007, Modelo de Evolução Geológica da Região do Atual Município de Atibaia (SP) Durante o Cenozóico: Revista UnG – Geociências, **6**, 1, 4–31.

Evjen, H. M., 1938, Depth factors and resolving power of electrical measurements: Geophysics, **3**, 2, 78–95, doi: 10.1190/1.1439485.

Gallas, J. D. F., 1990, Modelamento analógico de polarização induzida para corpos cilíndricos e tabulares, 117p. M.S. dissertation, Centro de Geociências, Universidade Federal do Pará – UFPA, Brazil.

Gallas, J. D. F., 2000, Principais Métodos Geoelétricos e suas Aplicações em Prospecção Mineral, Hidrogeologia, Geologia de Engenharia e Geologia Ambiental. Rio Claro, 174p. Tese (Doutorado em Geociências e Meio Ambiente) - Instituto de Geociências e Ciências Exatas, Universidade Estadual Paulista - Unesp.

Gallas, J. D. F., and Verma, O. P., 2006, Resistividade e polarização induzida (IP) – modelagem analógica: Revista Brasileira de Geofísica, **24**, 1, 25–35, doi: 10.1590/S0102-261X2006000100002.

Hallof, P. G., 1957, On the interpretation of resistivity and induced polarization measurements: Cambridge, MIT, Ph. D. thesis, 216p.

Hallof, P. G., 1967, Theoretical induced polarization and resistivity studies scale model cases. Ontario, Canada, McPhar Geophysics Limited, 1967, 106p.

Hallof, P. G., 1968, Theoretical induced polarization and resistivity studies scale model cases, phase II. Ontario, Canada, McPhar Geophysics Limited, 73p.

Hallof, P. G., 1970, Theoretical induced polarization and resistivity studies scale model cases, phase III. Ontario, Canada, McPhar Geophysics Limited, 133p.

Hasui, Y., and Oliveira, M. A. F., 1984, Província Mantiqueira – Setor Central, *in* Almeida, F.F.M., Hasui, Y. (Coord.), O Pré-Cambriano do Brasil. São Paulo: Edgar Blücher, p. 308–344.

IPI2WIN-1D Program, 2000, Programs set for 1-D VES data interpretation. Dept. of Geophysics, Geological Faculty, Moscow University, Russia.

Keller, G. V. and Frischknecht, F. C., 1966, Electrical methods in geophysical prospecting. Oxford: Pergamon Press, 517 p.

Leal, C. A., 2007, Geofísica aplicada na Avaliação de Recursos Hídricos Subterrâneos e Meio Ambiente da Zona Costeira do Campo Petrolífero de Fazenda Alegre, Norte Capixaba – Espírito Santo, 181p. M.S. dissertation, Universidade Federal do Ceará - UFC, Instituto de Ciências do Mar, Post-Graduate Program in Tropical Marine Sciences.

Muskat, M., and Evinger, H. M., 1941, Current penetration in direct current prospecting: Geophysics, **6**, 397–427, doi: 10.1190/1.1443734.

Oliva, A. and Chang, H. K., 2007, Mapeamento do Lençol Freático no Município de Rio Claro (SP) Empregando a Técnica da Sondagem Elétrica Vertical: Geociências, **26**, 1, 27–34.

Orellana, E., 1972, Prospeccion geoeletrica en corriente continua. Madrid: Paraninfo, 523 p.

Roy, A., 1972, Depth of investigation in Wenner, three-electrode and dipole-dipole DC resistivity methods: Geophysical Prospecting, **20**, 329–340, doi: 10.1111/j.1365-2478.1972.tb00637.x.

Roy, A., and Apparao, A., 1971, Depth of investigation in direct current methods: Geophysics, **6**, 5, 943–959, doi: 10.1190/1.1440226.

Rucker, D. F., C.-H. Tsai, K. C. Carroll, S. Brooks, E. M. Pierce, A. Ulery, and C. Derolph, 2021, Bedrock architecture, soil texture, and hyporheic zone characterization combining electrical resistivity and induced polarization imaging: J. Applied Geophysics, **188**, 104306. doi: 10.1016/j.jappgeo.2021.104306.

Silva, D. D., 2014, Caracterização de Áreas Favoráveis à Extração de Blocos Graníticos de Grande Porte com o Uso da Eletrorresistividade: M.S. dissertation in Geology, Instituto de Geociências, Universidade de São Paulo, SP, Brazil, 92 p.

Ward, S. H., 1990, Resistivity and induced polarization methods, *in* Ward, S.H., ed., Geotechnical and Environmental Geophysics, **1**: Review and Tutorial, Tulsa: Society of Exploration Geophysicists (SEG), chapter 6, 147–189, doi: 10.1190/1.9781560802785.ch6.

Zhody, A. A. R., 1989, A new method for automatic interpretation of Schlumberger and Wenner sounding curves: Geophysics, **54**, 245–253, doi: 10.1190/1.1442648.

Gallas, J.D.F.: manuscript elaboration in its entirety, including field acquisition, processing and data interpretation of a real case of the use of applied geophysics to support a housing project.

Received on January 21, 2022 / Accepted on June 07, 2022